Hydrothermal synthesis of CeO_2 nano-particles

A.I.Y. Tok*, F.Y.C. Boey, Z. Dong, X.L. Sun

School of Materials Science & Engineering, Nanyang Technological University, Nanyang Avenue, 639798 Singapore, Singapore

** Corresponding author. Tel.: +65 67904935; fax: +65 67904935.*

Abstract

Nano-crystalline particles of CeO_2 have been synthesized via a low temperature hydrothermal synthesis process. Two types of precursors were studied—cerium hydroxide and ceria acetate. The precursors were adjusted to a basic (pH 10) and acidic (pH 4) medium before hydrothermal treatment at various durations of 6, 12, 18, and 24 hat 250°C using a Teflon-lined hydrothermal bomb. The synthesized samples were characterized using DTA/TGA, XRD and TEM. Based on the characterization results, both precursor systems produced crystalline ceria nano-particles after 6 h of hydrothermal synthesis at 250 °C. The average crystallite sizes were 6 and 15 nm for the hydroxide and acetate system, respectively. The acetate precursor system appeared to produce better particles in terms of crystallinity and morphology. Based on the DTA/TGA analysis, hydrothermal synthesis had been effective in reducing the amount of intermediate products. With increasing hydrothermal treatment duration of up to 24 h, the samples did not exhibit a remarkable improvement in properties. The synthesized nano-particles were subsequently heat treated at 500 and 1000°C for 2 h. After the heat treatment, enhanced crystallinity and growth in crystallite size was observed, but particles appeared more agglomerated.

Keywords: Hydrothermal synthesis; CeO_2; Nano-particles; Rare earth oxide

1. Introduction

Rare earth oxide nano-particles have exceptional luminescence, magnetic and electronic properties due to their unfilled 4f electronic structure. As such, rare earth-based phosphors, magnetic materials, hydrogen storage material and high surface area support catalyst are being widely developed. Most of the applications require the use of non-agglomerated nano-particles, as aggregated nano-particles lead to inhomogeneous mixing, poor sinterability and compromised quantum properties [1]. However, nano-crystallites with a primary particle size <5 nm have a stronger tendency to agglomerate, making processing very difficult. As such, the benefits expected from highly crystalline nano-particles are easily lost during the manufacture of components unless weakly agglomerated nano-particles can be produced [2].

Ceria (CeO_2) is widely used as an oxygen ion conductor in solid oxide fuel cells, oxygen pumps and amperometric oxygen monitors because of its high oxygen ion conductivity [3–8]. Ceria has also received much success in redox and combustion catalysts due to its ability to shift between reduced and oxidized state as a result of change in gas phase oxygen concentration [9]. As an oxygen storage component, ceria act as an oxygen buffer providing oxygen under lean conditions and removing it under rich conditions for optimal conversion in three-way catalyst system [4,5]. Under working conditions, the catalysts are exposed to alternating O_2 deficient to excess O_2 environment. Ceria, in this situation, has the ability to donate its oxygen for the removal of CO and hydrocarbons during the O_2 deficient part of the cycle while absorbing and storing oxygen from O_2, NO and water during the excess O_2 environment [6]. This unique feature of ceria is thus termed as oxygen storage capacity (OSC). It derives from the ability to be easily and reversibly reduced to several CeO_2-x stoichiometries when exposed to O_2 deficient atmospheres [6].

Hydrothermal processing studies on the synthesis of nano-particles have focused on particle size, morphology and crystal polymorph. The pH of the reaction medium is a significant parameter affecting the nature and crystallinity of the nano-particles. Wu et al. [10] reported on the effects of pH of the reaction medium on the crystallization of ceria grains under hydrothermal conditions when cerium hydroxide was used as the precursor.

The synthesis mechanism was thought to be by Ostwald ripening, where in an acidic medium and with the dissolution of the precursor, grain growth is faster in contrast to a basic medium.

This paper describes the hydrothermal synthesis of CeO_2 nano-particles derived from two types of precursors—cerium hydroxide and ceria acetate, discusses the thermal degradation of the precursors as well as the effects of synthesis duration on the crystallinity and morphology of the nano-particles.

2. Experimental procedure

Hydrothermal synthesis was employed to synthesize cerium oxide nano-particles from two types of precursors (cerium hydroxide and ceria acetate), and the effects of hydrothermal time and subsequent heat treatment were studied. Raw materials used were cerium carbonate ($Ce_2(CO_3)_3 \bullet 3H_2O$, Ce_2O_3/TREO 60.5%), hydrous cerium oxide stabilized by acetate ions ($CeO_2 \bullet {}_xH_2O$), both from Advanced Materials Resources, acid (65% HNO_3), acetic acid (100% CH_3COOH), ammonia hydroxide (28% NH_3) and hydrogen peroxide (30% H_2O_2), all of which were from Merck. In stock solution preparation, cerium carbonate was dissolved in nitric acid to yield cerium(III) nitrate, hydrous cerium oxide stabilized by acetate ions (cerium acetate gel) was dissolved in deionized water to yield 'acetate stabilized colloidal ceria' and will be identified as ceria acetate for the following discussions. Ammonia hydroxide was diluted to 7 M to be used as the precipitating agent and the adjustment of pH. The synthesis was done using a 45 ml PTFE-lined Acid Digestion Bomb from Parr Instrument Company.

2.1. Cerium(IV) hydroxide precursor

Cerium(III) nitrate, $Ce(NO_3)_3 \cdot 6H_2O$, was diluted to $[Ce^{4+}]$ = 0.5 M using deionized water. Hydrogen peroxide in the molar ratio (H_2O_2:Ce^{4+}) of 1:2 was added to cerium(III) nitrate solution and stirred for 5 min under heat on a magnetic hotplate to convert Ce^{3+} to Ce^{4+}. Diluted ammonia solution (7 M) in the molar ratio (NH_4OH:Ce^{4+}) of 3 was then added to this mixture. Upon adding ammonia solution, the precipitation reaction occurred. Excess ammonia solution was added drop-wise until a pH of 8.8 was achieved. The mixture was left to stir continuously at 80°C for 1 h for the reaction to complete.

After an hour, the pale yellow precipitates ($Ce(OH)_4$) were washed several times with deionized water until the conductivity of the supernatant solution was less than or equal to 2 milli-Siemens (mS). After adjusting to pH 10 using ammonia solution, 30 ml of the washed precipitates were placed into the Teflon vessel of the hydrothermal bomb. The bomb was then placed in the oven and heated at the respective durations (0–24 h). The final products were re-washed with deionized water to achieve conductivity of less than or equals to 2 mS, and dried at 75°C. Dried powders were ground and set aside for heat treatment or characterization.

2.2. Ceria acetate precursor

Ceria acetate was diluted to $[Ce^{4+}]$ = 0.5 M using deionized water. The conductivity and pH of the solution were noted before placing 30 ml of the solution into the Teflon vessel. The bomb was then placed in the oven and heated to 250°C at different treatment times. After recovery of the final products, conductivity and pH of the products were recorded. The products were later centrifuged and dried at 75°C. Dried powders were ground and set aside for heat treatment and characterization.

XRD analysis (Shimadzu 6000) was used to determine the phase composition and to estimate the crystallite size of the nano-particles. Cu Kα radiation in the 2θ range of 20–80° at 4° 2θ/min was used for measurement. The crystallite size of the powders was estimated using the Scherrer equation:

$$D_{hkl} = \frac{0.89\lambda}{\beta_{hkl} \cos\theta} \quad (1)$$

where λ is the wavelength of the incident X-rays (0.15406 nm); θ the diffraction angle; β_{hkl} the measured half-width.

Lattice parameter (a) was calculated by the following lattice parameter formula (Eq. (2).

$$d = \frac{a}{\sqrt{h^2 + k^2 + l^2}} \quad (2)$$

a refers to the CeO_2 FCC lattice parameter, and *h*, *k*, *l* are the crystalline face indexes while *d* is the crystalline face space.

Powder morphology, state of agglomeration and crystalline state were observed via TEM (Jeol JEM 2010).

Differential thermal analysis and thermo-gravimetric analysis (TG-DTA, Netzsch STA 449C) was done in dry-air atmosphere up to 1000°C using a heating rate of 10 °C/min.

3. Results and discussion

The DTA/TG spectrum in Fig. 1 shows the thermal decomposition process for the cerium(IV) hydroxide. The total measured weight loss from 25 to 900°C was 11.64%, while the theoretical weight loss for the decomposition of cerium hydrate oxide is 17.3%, i.e. $Ce(OH)_4$/ $CeO_2 \bullet 2H_2O$ to CeO_2.

$Ce(OH)_4$ is a hydrous oxide, represented by $CeO_2 \bullet {}_xH_2O$ which dehydrates progressively. Therefore, the decomposition of the precursor is a form of dehydration process of the hydrated CeO_2. It is suggested that the difference in weight loss observed could be due to the following reasons: (a) precipitate consisting of a partially hydrated form of ceria, (i.e. $CeO_2 \bullet {}_xH_2O$), for which a 11.64% weight loss on decomposition corresponds to x = 1.35 or (b) the precipitate consisted of a mixture of phases like $CeO_2 \bullet 2H_2O$+ CeO_2 [2].

The DTA/TG traces for ceria acetate precursor are shown in Fig. 2. The precursor measured a total weight loss of 12.55% with four distinct temperature peaks. The theoretical weight loss to be observed for pure cerium acetate with the chemical formula of $Ce(CH_3COO)_3 \bullet 1.5H_2O$ is 50% [11]. However, it is not expected for the precursor used in this study to have similar weight loss but the acetate groups will still undergo similar chemical reactions thermally. The first endothermic peak was detected at around 100 °C. This is attributed to the release of the water molecules present in the precursor. From 100 to 200 °C, the weight loss was attribute to the removal of the surface acetate groups and later the formation of the acetic acid when surface acetate hydrolysis occurs [12]. This also explains the very weak endothermic peak detected at 200 °C. There was a sharp

weight loss from 200 to 400°C and a corresponding exothermic peak. This exothermic peak suggests the formation of oxyacetate and dioxocarbonate complexes with cerium, $Ce(OH)(CH_3COO)$ and $Ce_2O_2CO_3$. The formation of these complexes during thermal decomposition have been reported for the Lanthanide acetates [11,12]. As temperature increased to 700 °C, the $Ce_2O_2CO_3$ decomposed endothermally to produce the final product, CeO_2 suggesting that the complete formation on CeO_2 occurs after 700 °C.

In Fig. 3, after 6 and 24 h of hydrothermal treatment, weight loss is dramatically reduced to 2.64 and 1.37%. The distinct temperature peaks are similar to that of the precursor. However, the distinct exothermic peak for the hydrothermal treated samples is no longer as pronounced as that of the precursor. This could be due to the amount of acetate complexes formation being reduced considerably after hydrothermal treatment. Traces of cerium acetate complexes were still present in the samples after hydrothermal treatment. The amount is however, significantly lower than that found in the precursor.

Figs. 4 and 5 show the XRD patterns of the ceria produced from cerium(IV) hydroxide precursor and ceria acetate precursor, respectively, at various hydrothermal treatment durations. Figs. 6 and 7 show their lattice constant values, respectively. In Fig. 4, the nano-particles exhibited some degree of crystallinity and displayed all of the major peaks of CeO_2 with a cubic structure (JCPDF 34-0394) after 6 h treatment. However, no significant improvement in crystallinity was observed between 6 and 24 h, and the peaks were broad with weak intensities. This trend is similar with the ceria acetate system. However, the peaks are significantly narrower with higher intensities suggesting larger crystallite sizes at an average of 15.5 nm as calculated and larger degree of crystallinity as compared to the cerium(IV) hydroxide system. The peaks at higher 2θ angles can also be clearly observed for all samples.

The lattice constants were calculated using Rietveld refinement method (Topas software), and the obtained data are included in Table 1. For CeO_2 obtained using $Ce(OH)_4$ precursor, the lattice parameter decreased by about 0.2% after hydrothermal treatment at 250°C for 6 h (Fig. 6). When the treatment duration increased from 6 to 12 h at the same temperature, the lattice expanded. The lattice constant only varied within a narrow range ($|\Delta a|/a \approx 0.03\%$) after 12 h, indicating that the structure became stable. For

CeO_2 samples obtained using ceria acetate precursor, the lattice constant decreased by about 0.5% after hydrothermal treatment at 250°C for 6 h as shown in Fig. 7. Further changes of lattice constant were very small when treatment duration was increased. The variation of lattice constant was less than 0.03%.

From Table 1, it can be seen that crystallite size remained relatively constant with respect to the change in hydrothermal treatment time. The crystallite size of the ceria acetate precursor is half the size of the hydrothermal treated crystallite sizes. It appears that hydrothermal treatment did contribute to the growth in crystallite size and increase in crystallinity of the precursors.

Both precursors employed were in the form of $CeO_2 \cdot_x H_2O$. Acetate anion groups used to stabilize the ceria for the ceria acetate gel dissociated easily in the form of acetic acid; dissociation of acetic acids occurs very easily. Similarly, the use of acetate-based precursors reduced the time needed to achieve the same degree of crystallinity under the same hydrothermal conditions.

Hydroxide precursors underwent the hydrothermal crystallization mechanism, where precipitated solid hydroxide samples are placed into the hydrothermal autoclave and further transformed into its oxide form. The hydroxide precipitates will experience a dissolution–re-precipitation process or the Ostwald ripening process. It has been reported that pH of the medium used in hydrothermal synthesis has a critical and significant influence in the crystallinity of the final products [10].

When Ostwald ripening occurs, smaller grains dissolve faster, the diffusion of solute is slower and larger grains grow more slowly. Hence, it can be assumed that the growth kinetics is controlled by diffusion or surface reaction. This is true for substances where their solubility products are big such as K_{sp} (AgCl) = 1.8 x 10^{-10} and K_{sp} ($BaSO_4$) = 1.1 × 10^{-10}. However, the solubility product of $Ce(OH)_4$ is 2 x 10^{-48} and is much smaller than the precipitated substances. Therefore, an opposite phenomenon where smaller grains dissolved slower with the solute diffusing faster and larger grains growing more quickly is observed. Thus, it is assumed the growth kinetics is controlled by dissolution.

$Ce(OH)_4$ is a basic precipitate, therefore increasing $[OH^-]$ will result in a decrease in solubility of $Ce(OH)_4$ and increasing $[H^+]$ will result in a dramatic increase in solubility of $Ce(OH)_4$. For Ostwald ripening, there is an equilibrium value for grain size, r^*. When r is smaller than r^*, smaller grains will dissolve and disappear. When r is greater than r^*, larger grains will continue to grow. Under a basic medium, concentration of hydroxide ions becomes very high with small solubility values of $Ce(OH)_4$, the dissolution of the precursor grains become very limited. Hence, Ostwald ripening proceeds to a very small extent, and the size of the grains increased only slightly. The opposite would have occurred if the medium was adjusted to acidity.

Figs. 8 and 9 show the XRD patterns for the 24 h-synthesized ceria from cerium(IV) hydroxide and ceria acetate precursors, respectively, heat treated at 500 and 1000°C with holding time of 2 h. In both figures, it can be seen that the characteristic peaks are sharper and narrower. The higher 2θ peaks for the hydroxide system can also be observed after heat treatment. This crystallite size after heat treatment at 500 and 1000°C grew to 8.8 and 47.4 nm, respectively. In comparison, the samples from the ceria acetate system exhibited a larger degree of crystallinity than cerium hydroxide system. The crystallite size for the ceria acetate system after heat treatment was 17.7 and 53.6 nm at 500 and 1000 °C, respectively.

The ceria synthesized from cerium(IV) hydroxide in Fig. 10 (a) after 24 h hydrothermal treatment exhibited very fine particles, which were agglomerated. Crystallinity could be observed based on the particles and its corresponding electron diffraction pattern. Its crystallite size is about 5–6 nm as estimated from the TEM micrographs. The particles generally shown rounded edges but they are not well-defined due to its small size.

For the ceria synthesized from the acetate system after 24 h in Fig. 10 (b), particles are very well-defined and relatively dispersed. Good crystalline faces and crystallinity state could be observed. The particle sizes, at about 10–15 nm, are slightly bigger compared to the cerium(IV) hydroxide system, agrees well to the calculated crystallite sizes using the XRD results. The ceria acetate system appears to be less agglomerated than the cerium(IV) hydroxide system. However, agglomeration of the particles still appears to be a problem.

4. Conclusion

Nano-particles of ceria have been synthesized using low temperature hydrothermal synthesis. Cubic-fluorite ceria structure can be easily hydrolyzed under hydrothermal conditions in 6 h at 250°C with relatively good crystallinity. Small crystallite sizes in the range of 6–15 nm were obtained and they appeared to be independent on the hydrothermal treatment times at the given temperature. The choice of precursors in the synthesis of ceria has yielded relatively different results in terms of crystallinity, crystallite size and specific surface area. The ‘acetate stabilized colloidal ceria’ has been able to give particles with good crystallinity and good morphology when viewed under the TEM. Both ceria systems experienced relatively agglomerated particles when synthesized under hydrothermal conditions. Further studies and experiments are being done to reduce the agglomeration of the nano-particles via the use of surfactants.

References

[1] Y. Chen, N. Glumac, B.H. Kear, G. Skandan, Nanostruct. Mater. 9 (1997) 101–104.

[2] B. Djuricic, S. Pickering, J. Eur. Ceram. Soc. 19 (1999) 1925–1934.

[3] M. Hirano, E. Kato, J. Am. Ceram. Soc. 79 (1996) 777–780.

[4] S. Colussi, C. de Leitenburg, G. Dolcetti, A. Trovarelli, J. Alloys Compd. 374 (2004) 387–392.

[5] T. Masui, T. Ozaki, K. Machida, G. Adachi, J. Alloys Compd. 303–304 (2000) 49–55.

[6] A. Trovarelli, M. Boaro, E. Rocchini, C. de Leitenburg, G. Dolcetti, J. Alloys Compd. 323–324 (2001) 584–591.

[7] M. Boaro, A. Trovarelli, J.H. Hwang, T.O. Mason, Solid State Ionics 147 (2002) 85–95.

[8] L.F. Liotta, G. Pantaleo, A. Macaluso, G. Marcì, S. Gialanella, G. Deganello, J. Sol–Gel Sci. Technol. 28 (2003) 119–132.

[9] A. Trovarelli, Catal. Rev. Sci. Eng. 38 (1996) 439–509.

[10] N.C. Wu, E.W. Shi, Y.Q. Zheng, W.J. Li, J. Am. Ceram. Soc. 85 (2002) 2462–2468.

[11] M.J. Fuller, J. Pinkstone, Thermal Analysis of the Oxalate Hexahydrates and Decahydrates of Yttrium and the Lanthanide Elements, J. Less-Common Metals 70 (1980) 127.

[12] G.A.M. Hussein, Powder Technol. 118 (2001) 285–290.

List of Tables

List of Figures

Table 1

Starting materials	Treatment time (h)	As synthesized			Heat treated at 500 °C			Heat treated at 1000 °C		
		Lattice type	Lattice constant	D_{hkl} (nm)	Lattice type	Lattice constant	D_{hkl} (nm)	Lattice type	Lattice constant	D_{hkl} (nm)
$Ce(OH)_4$	Precursor	Amorphous	5.4257	5.5	–	–	–	–	–	–
$Ce(OH)_4$	6	Cubic	5.4152	5.5	–	–	–	–	–	–
$Ce(OH)_4$	12	Cubic	5.4208	5.9	–	–	–	–	–	–
$Ce(OH)_4$	18	Cubic	5.4226	6.7	–	–	–	–	–	–
$Ce(OH)_4$	24	Cubic	5.4221	6.0	Cubic	5.4094	8.8	Cubic	5.4068	8.8
Ceria acetate	Precursor	Amorphous	5.4339	6.14	–	–	–	–	–	–
Ceria acetate	6	Cubic	5.4075	13.8	–	–	–	–	–	–
Ceria acetate	12	Cubic	5.4061	15.4	–	–	–	–	–	–
Ceria acetate	18	Cubic	5.4073	15.8	–	–	–	–	–	–
Ceria acetate	24	Cubic	5.4068	17.2	Cubic	5.4071	17.7	Cubic	5.4065	17.7

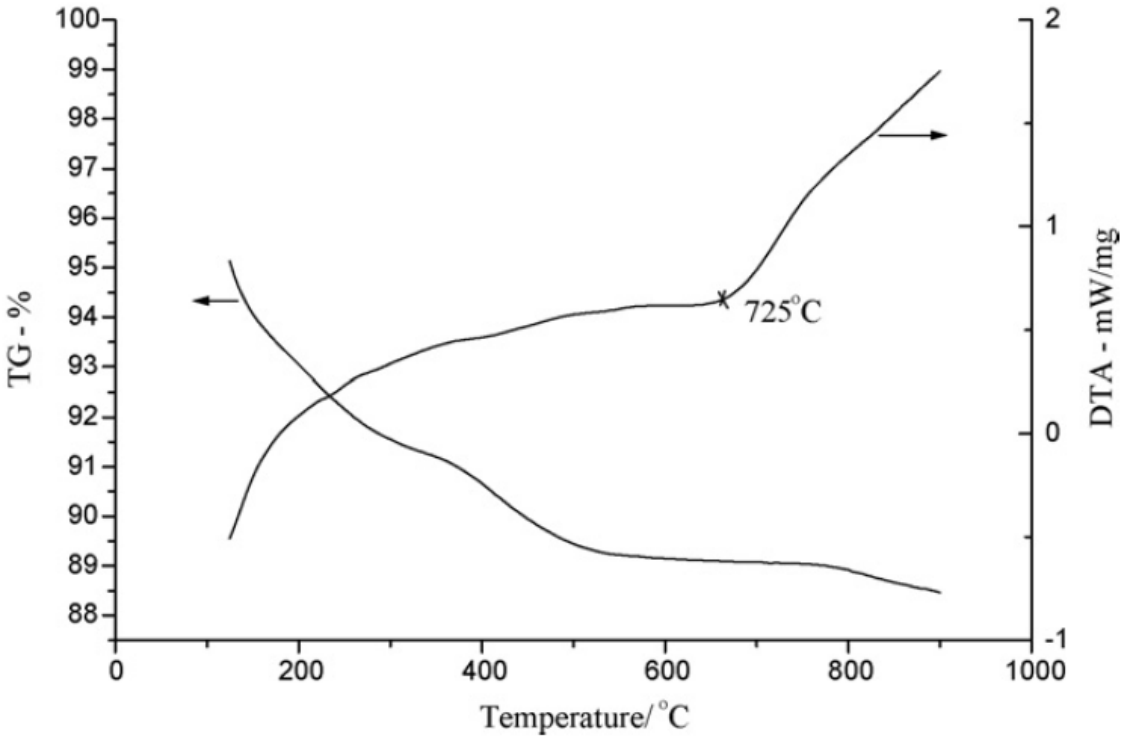
100
99
98
97
96
95
94
93
92
91
90
89
88
TG - %
2
1
0
-1
DTA - mW/mg
725°C
0
200
400
600
800
1000
Temperature/ °C

Fig. 1

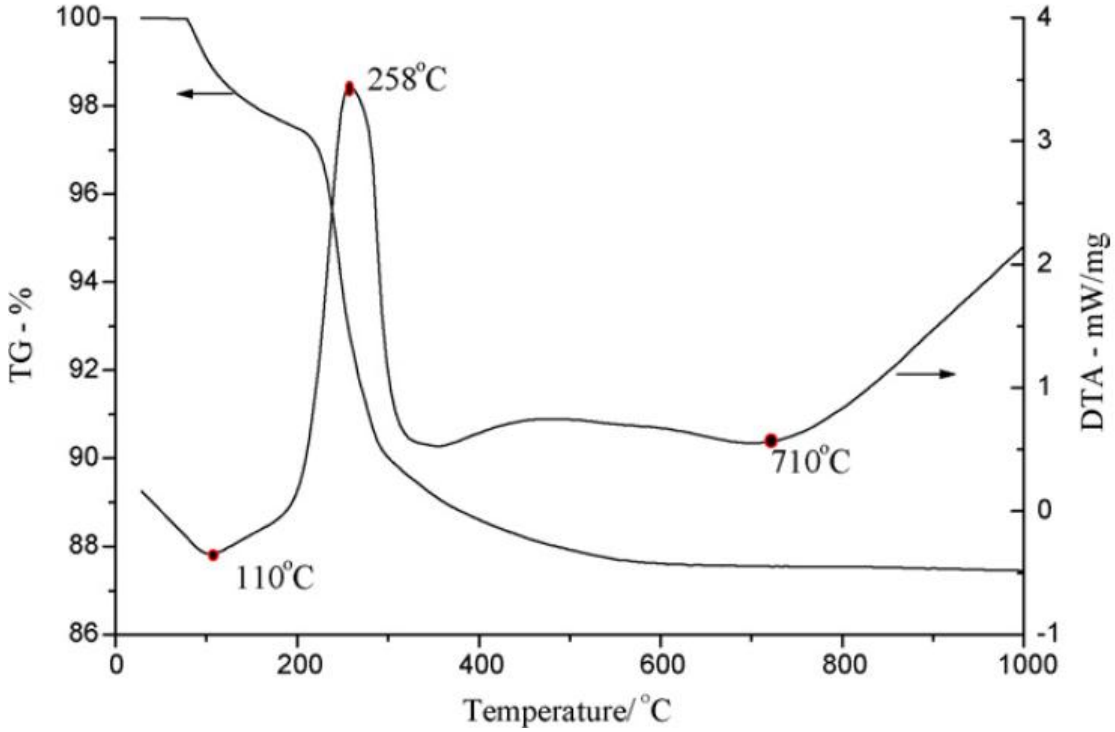
100
98
96
94
92
90
88
86
TG - %
4
3
2
1
0
-1
DTA - mW/mg
0
200
400
600
800
1000
Temperature/ °C
258°C
110°C
710°C

Fig. 2

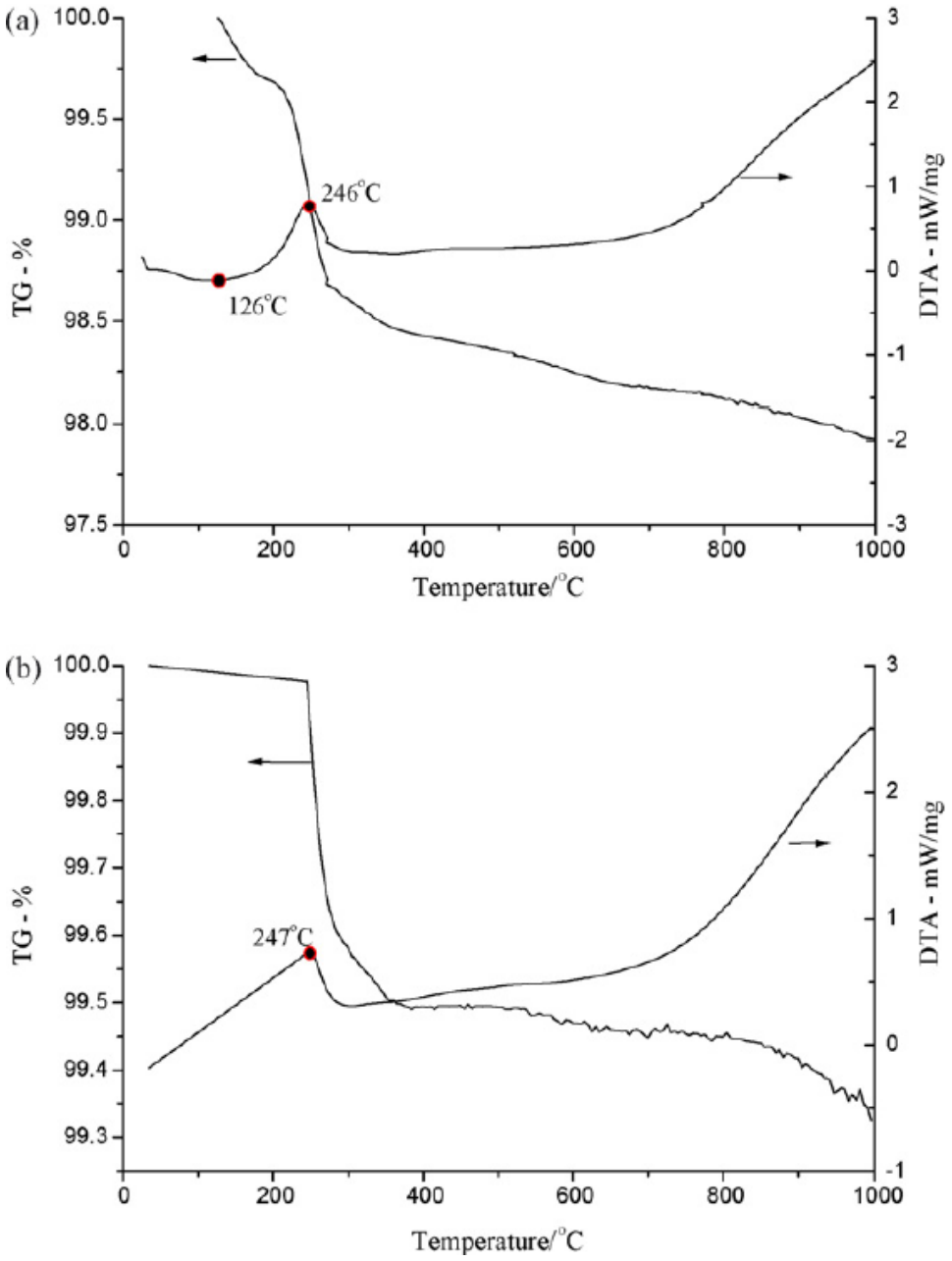
(a)
100.0
99.5
99.0
98.5
98.0
97.5
TG - %
246°C
126°C
3
2
1
0
-1
-2
-3
DTA - mW/mg
0
200
400
600
800
1000
Temperature/°C
(b)
100.0
99.9
99.8
99.7
99.6
99.5
99.4
99.3
TG - %
247°C
3
2
1
0
-1
DTA - mW/mg
0
200
400
600
800
1000
Temperature/°C

Fig. 3

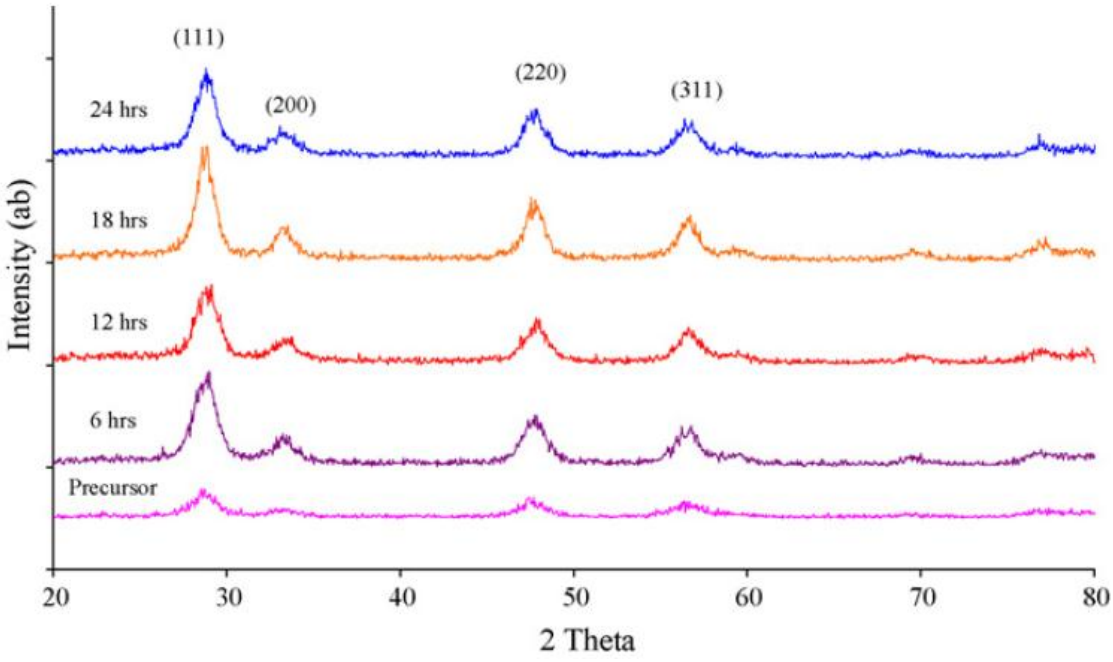
(111)
(200)
(220)
(311)
24 hrs
18 hrs
12 hrs
6 hrs
Precursor
Intensity (ab)
20
30
40
50
60
70
80
2 Theta

Fig. 4

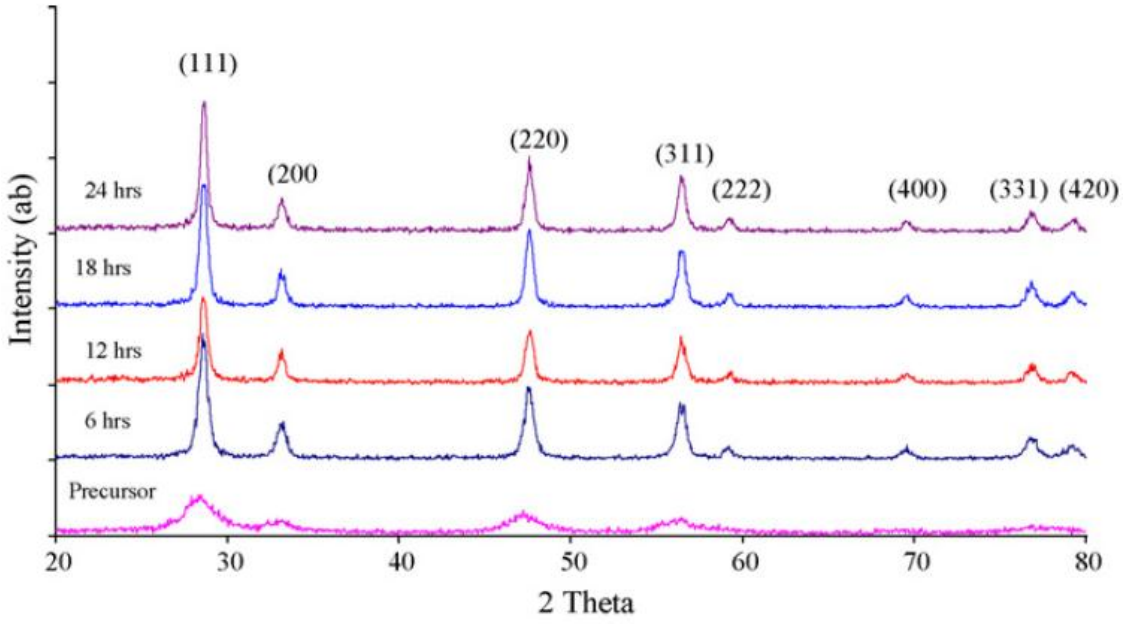
(111)
(200
(220)
(311)
(222)
(400)
(331)
(420)
24 hrs
18 hrs
12 hrs
6 hrs
Precursor
Intensity (ab)
20
30
40
50
60
70
80
2 Theta

Fig. 5

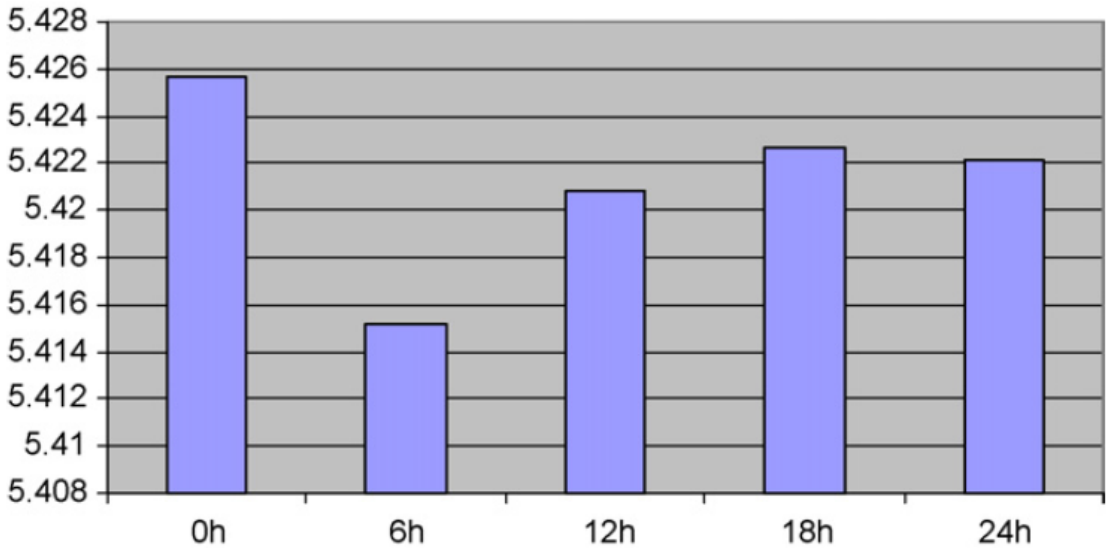
5.428
5.426
5.424
5.422
5.42
5.418
5.416
5.414
5.412
5.41
5.408
0h
6h
12h
18h
24h

Fig. 6

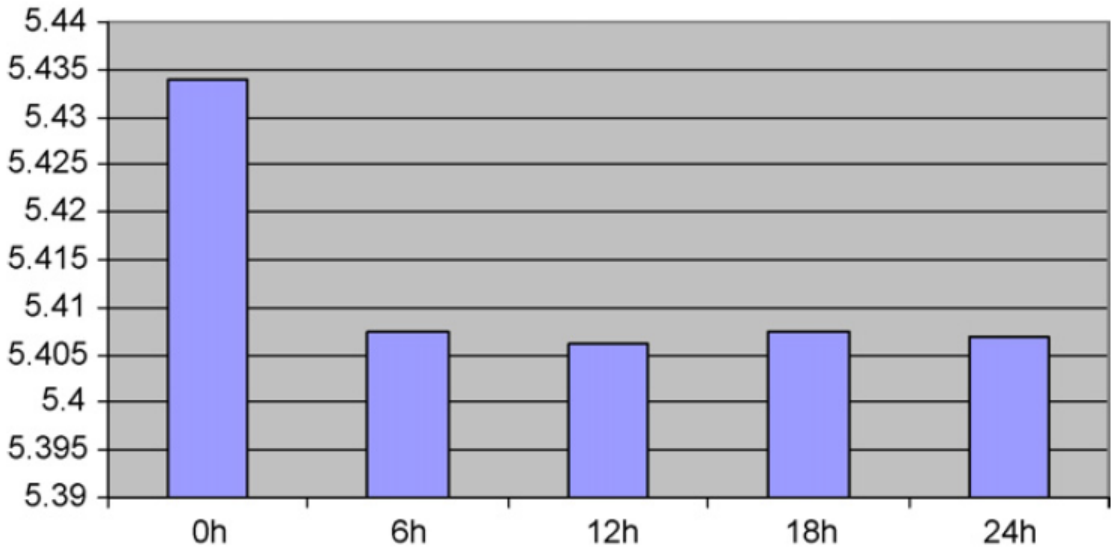
5.44
5.435
5.43
5.425
5.42
5.415
5.41
5.405
5.4
5.395
5.39
0h
6h
12h
18h
24h

Fig. 7

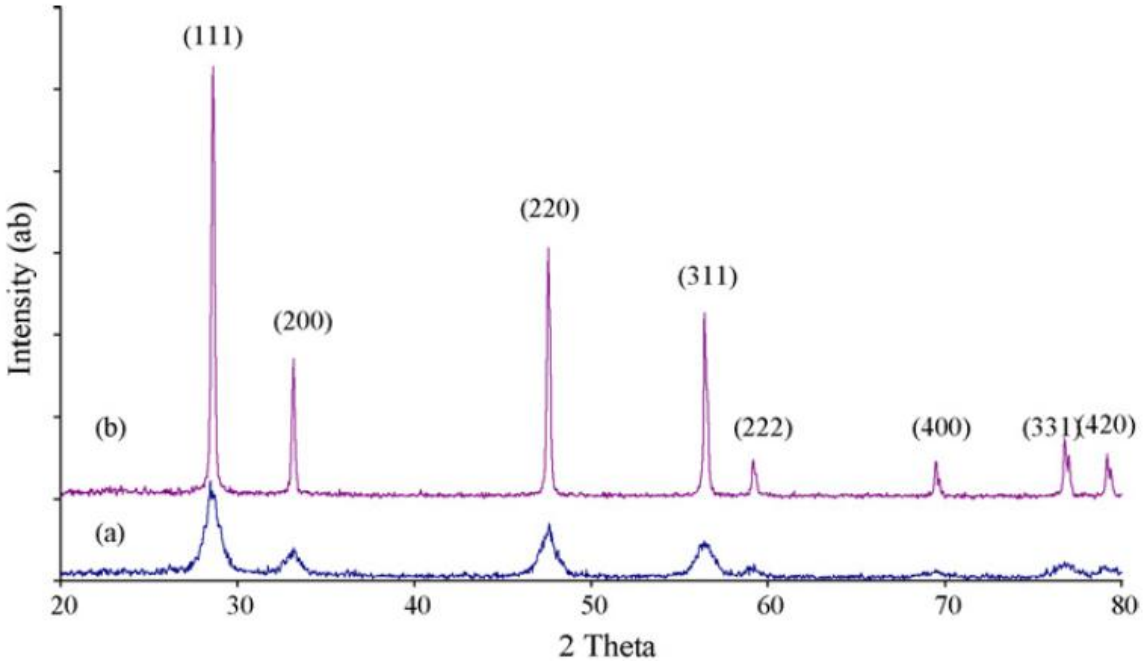
(111)
(200)
(220)
(311)
(222)
(400)
(331)
(420)
(b)
(a)
Intensity (ab)
20
30
40
50
60
70
80
2 Theta

Fig. 8

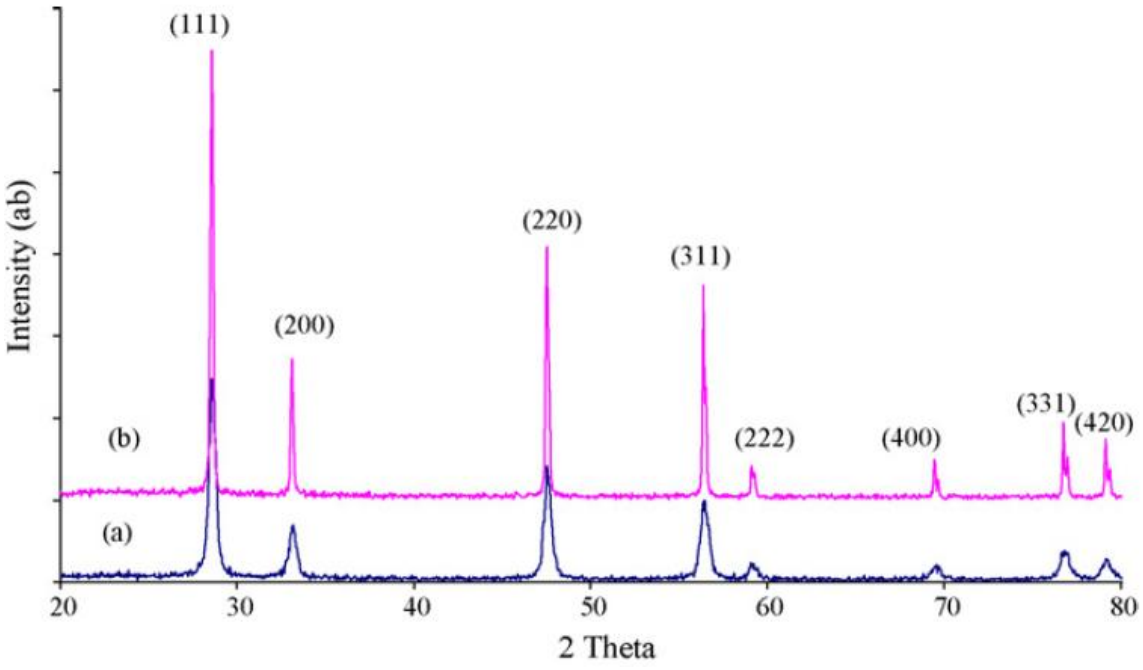
(111)
(200)
(220)
(311)
(222)
(400)
(331)
(420)
(b)
(a)
Intensity (ab)
20
30
40
50
60
70
80
2 Theta

Fig. 9

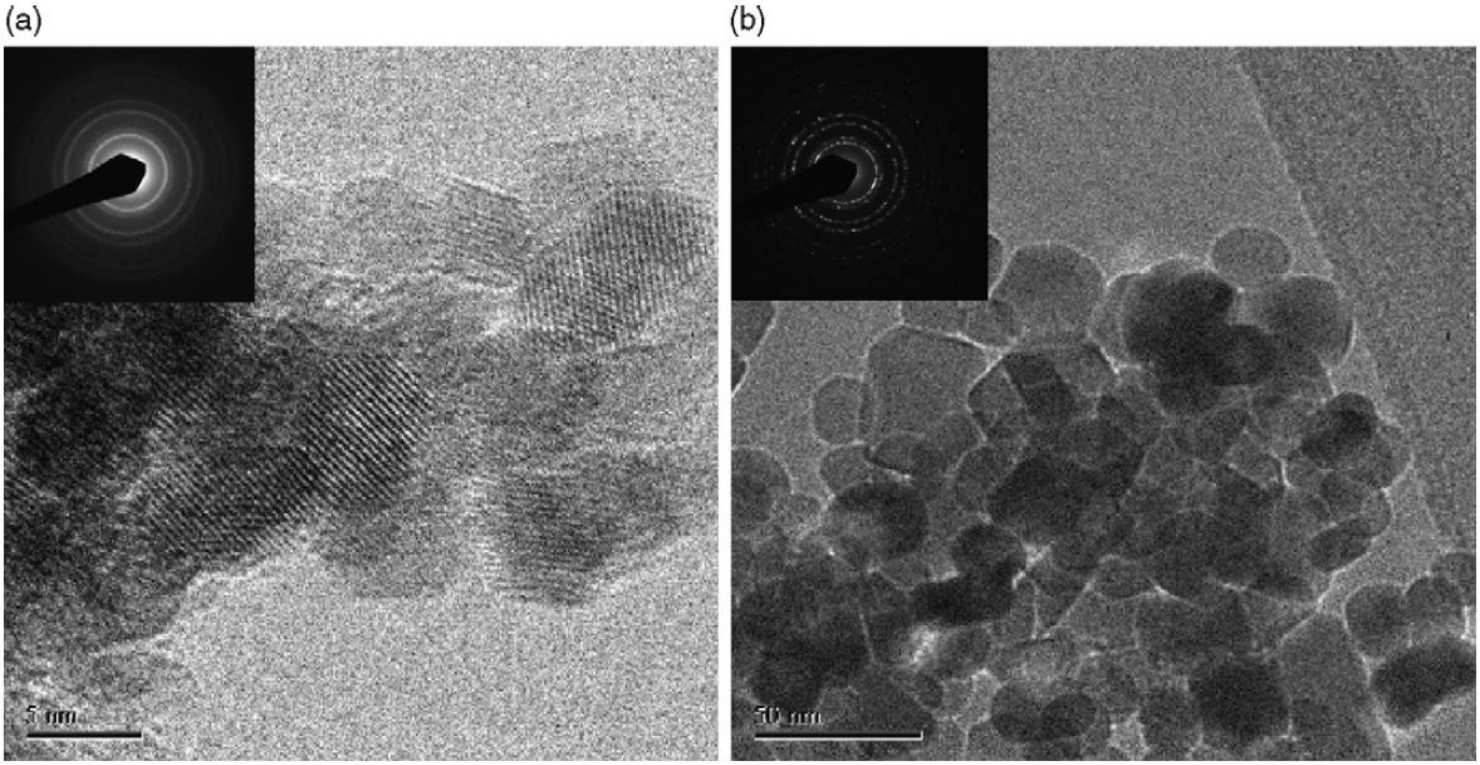

Fig. 10